

ROTATING ANTENNA MICROWAVE IMAGING SYSTEM FOR BREAST CANCER DETECTION

M. O'Halloran, M. Glavin, and E. Jones [†]

College of Engineering and Informatics
National University of Ireland Galway
University Road, Galway, Ireland

Abstract—Breast imaging using Confocal Microwave Imaging (CMI) has becoming a difficult problem, primarily due to the recently-established dielectric heterogeneity of normal breast tissue. CMI for breast cancer detection was originally developed based on several assumptions regarding the dielectric properties of normal and cancerous breast tissue. Historical studies which examined the dielectric properties of breast tissue concluded that the breast was primarily dielectrically homogeneous, and that and that the propagation, attenuation and phase characteristics of normal breast tissue allowed for the constructive addition of the Ultra Wideband (UWB) returns from dielectric scatterers within the breast. However, recent studies by Lazebnik et al. have highlighted a very significant dielectric contrast between normal adipose and fibroglandular tissue within the breast. Lazebnik also established that there was an almost negligible dielectric contrast between fibroglandular and cancerous breast tissue at microwave frequencies. This dielectric heterogeneity presents a considerably more challenging imaging scenario, where constructive addition of the UWB returns, and therefore tumor detection, is much more difficult. Therefore, more sophisticated signal acquisition and beamforming algorithms need to be developed. In this paper, a novel imaging algorithm is described, which uses a rotating antenna system to increase the number of unique propagation paths to and from the tumor to create an improved image of the breast. This approach is shown to provide improved images of more dielectrically heterogeneous breasts than the traditional fixed-antenna delay and sum beamformer from which it is derived.

Received 10 July 2010, Accepted 29 July 2010, Scheduled 6 August 2010

Corresponding author: M. O'Halloran (martin.ohalloran@gmail.com).

[†] M. O'Halloran, M. Glavin, and E. Jones are also with Bioelectronics Research Cluster, National Centre for Biomedical Engineering Science (NCBES), National University of Ireland Galway, University Road, Galway, Ireland.

1. INTRODUCTION

X-ray mammography, coupled with comprehensive physical examinations and regular self-examinations, is currently the most effective screening method for the detection of breast cancer. Despite this, more than 40,000 women die annually in the United States from breast cancer, making it the leading cause of death in American women. Worldwide, the incidence of breast cancer has increased by 0.5% annually, with 1.35 to 1.45 million new cases projected by 2010 [1]. The primary limitation of X-ray mammography is the difficulty of imaging radiographically dense glandular tissue, especially common amongst younger women, motivating the development of alternate breast imaging modalities. Microwave Imaging (MI) is one of the most promising alternatives to X-ray mammography as a method for the early detection of breast cancer.

The physical basis for microwave imaging is the dielectric contrast between the constituent tissues of the breast and cancerous tissue at microwave frequencies. Three alternative active microwave imaging techniques are under development, Hybrid Microwave-Induced Acoustic imaging [2–4], Microwave Tomography [5–10] and Ultra-Wideband (UWB) Radar imaging [11–27].

Ultra-Wideband (UWB) Radar imaging, as proposed by Hagness et al. [11], uses reflected UWB signals to determine the location of microwave scatterers within the breast. While the performance of UWB imaging algorithms tends to degrade with increased dielectric heterogeneity, UWB imaging systems are non-ionizing, non-compressing, potentially low cost and offer high specificity. The Confocal Microwave Imaging (CMI) approach to microwave imaging involves illuminating the breast with a UWB pulse, recording the backscattered signals and then using these signals to identify and locate significant dielectric scatterers within the breast. Regions of high energy within the resultant images may suggest the presence of tumours due to the dielectric contrast that exists between normal and cancerous tissue. The CMI approach is based on several assumptions regarding the dielectric properties of normal and cancerous breast tissue. These assumptions include the following:

- There is a significant dielectric contrast between normal and cancerous breast tissue.
- Normal breast tissue is primarily dielectrically homogeneous.
- The dielectric properties of normal tissue are such that constructive addition of UWB backscattered signals is possible.

Early work on the measurement of the dielectric properties of breast tissue largely satisfied these assumptions [28–30]. However, a recent

study of the dielectric properties of adipose, fibroglandular and cancerous breast tissue has highlighted the dielectric heterogeneity of normal breast tissue [25,26]. Significantly, rather than the dielectric properties of normal breast tissue being homogeneous, Lazebnik et al. found a very significant dielectric contrast between normal adipose and fibroglandular tissue within the breast. The dielectric properties of adipose tissue were found to be lower than any previously published data for normal tissue. Conversely, the dielectric properties of fibroglandular tissue were found to be significantly higher than any previously published data for normal breast tissue. This heterogeneity of normal breast tissue had been considerably underestimated in earlier studies, and the difficulty this presents to existing UWB beamformers has been examined by the authors previously [22]. Two approaches have emerged to improving the performance of UWB imaging algorithms in this dielectrically heterogeneous environment:

- (i) The introduction of contrast agents to improve the dielectric difference between fibroglandular and cancerous tissue [21].
- (ii) Investigation of various antenna configurations and intelligent beamforming algorithms which are more robust to dielectric heterogeneity [33].

In this paper, a novel rotating-antenna system is presented in order to address the problem. The rotating antenna system increases the number of independent paths from transmitting to receiving antenna, thus increasing the received energy and therefore producing an improved image of any tumor present. The performance of the proposed rotating antenna system is compared to that of the traditional fixed antenna system. The remainder of the paper is organized as follows: Section 2 will review the recently-established dielectric heterogeneity of normal breast tissue; Section 3 will describe existing antenna configurations before presenting the rotating antenna approach; Section 4 will describe the test procedure and corresponding results; Finally, the conclusions and suggestions for future work are detailed in Section 5.

2. DIELECTRIC PROPERTIES OF THE BREAST

The dielectric properties (and heterogeneity) of breast tissue have been comprehensively described previously [22, 34], and are summarised here for completeness.

Many of the historical studies examining the dielectric properties of breast tissue have tended to focus on the dielectric contrast between normal breast tissue (including both adipose and fibroglandular tissue)

and cancerous tissue, rather than distinguishing between types of normal tissue and examining their respective dielectric properties in isolation. Chaudhary [30], Surowiec [29] and Joines et al. [28] all measured the dielectric properties of normal and cancerous breast tissues from 3 MHz and 3 GHz, 20 kHz to 100 MHz, and 50 MHz to 900 MHz respectively. Chaudhary found a significant dielectric contrast between normal and malignant tissue of 4.7 : 1 for conductivity and 5 : 1 for relative permittivity. Similarly, Joines found a contrast ratio of 3.8 : 1 for conductivity and 6.4 : 1 for relative permittivity. Surowiec found that the tissue at the infiltrating edge of the tumor had increased dielectric properties, suggesting that even quite small tumors could still induce significant microwave backscattering. While these studies established a significant dielectric contrast between normal and cancerous tissue, they did not examine the dielectric contrast between adipose and fibroglandular tissue.

One of the first studies to suggest that the breast may be more dielectrically heterogeneous was completed by Campbell and Land [35]. They measured the complex permittivity of female breast tissue at 3.2 GHz, and while once again noting a significant dielectric contrast between normal and cancerous tissue, they also suggested that the range of dielectric properties of normal tissue was much greater than established in previous studies. The heterogeneity of normal breast tissue was further confirmed by Meaney et al. [36] who noted that the average permittivity values of normal tissue at 900 MHz were significantly higher than those previously published in Joines et al.'s *ex vivo* study [28]. Meaney et al. suggested that breasts with a greater concentration of dense fibroglandular tissue tended to have higher average permittivity values than less dense breasts.

Finally, one of the most comprehensive examinations of the dielectric properties of normal breast tissue was undertaken by Lazebnik et al. The key attribute of Lazebnik et al.'s first study [25] was the histological categorisation of the tissue samples. Each sample under consideration was quantified in terms of the percentage of adipose, glandular and fibroglandular tissue present in the sample. These results of Lazebnik's study can be summarised as follows:

- (i) Adipose tissue has much lower dielectric properties than previously assumed.
- (ii) Conversely, fibroglandular tissue has much higher dielectric properties than previously thought.
- (iii) The dielectric heterogeneity of normal breast tissue was previously significantly underestimated.

The effect of this dielectric heterogeneity is very significant. The performance and robustness of most UWB beamforming algorithms

is highly dependent on the coherence of the backscattered signals from the tumor after time-alignment, and therefore their effectiveness is markedly reduced where there is a significant difference between the assumed homogenous channel model and the actual heterogeneous breast [22]. This prompts the development of more sophisticated imaging systems to compensate for the more challenging imaging environment of the dielectrically heterogeneous breast.

3. ANTENNA CONFIGURATIONS

Several different UWB imaging configurations have previously been considered. These different configurations include various antenna configurations and variations in how the reflections from the breast are recorded. Existing configurations are considered first, before the rotating antenna system proposed in this paper is described.

3.1. Existing Fixed Antenna Systems

Two antenna configurations have primarily been examined: The planar configuration first used by Hagness et al. [11] and the cylindrical configuration developed by Fear et al. [13]. A configuration is defined by both the orientation of the patient and the position of the antenna array. In the planar configuration, the patient is oriented in the supine position with a planar antenna array placed across the naturally

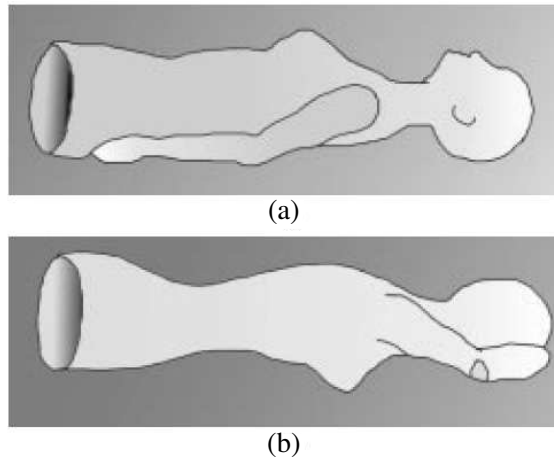


Figure 1. The supine patient position is shown in (a), while the prone patient position is shown in (b). This image is reproduced from [13].

flattened breast. Conversely, in the cylindrical configuration, the patient lies in the prone position with the breast naturally extending through an opening in the examination table. A cylindrical array of antennas surrounds the breast. Both prone and supine positions are shown in Figure 1.

The manner in which the backscattered energy is recorded in existing imaging algorithms is also of significant importance. These approaches can be divided into two categories: monostatic and multistatic. In the monostatic case, each antenna in the array sequentially illuminates the breast with a UWB pulse and that antenna alone also records the backscatter. Conversely, in the multistatic approach, the breast is once again sequentially illuminated by each antenna in the array, but this time the backscattered signals are recorded at all antenna array elements located at different positions around the breast. The multistatic approach has been shown to significantly outperform monostatic imaging algorithms for two specific reasons:

- The multistatic approach acquires many more reflections from any dielectric scatterer within the breast ($\frac{(N-1)^2}{2}$ signals in a multistatic system compared to N signals in a corresponding monostatic system with N antennas).
- The multistatic approach offers much greater spatial diversity in the propagation paths of the reflected signals, allowing for any dielectric scatterer to be more precisely localised.

In the following section, a novel rotating antenna approach is described, which seeks to further increase the number of unique recorded reflection and the spatial diversity of the propagation paths in multistatic systems to produce an improved microwave image of the breast.

3.2. Rotating Antenna System

The proposed system involves a circular array of antennas surrounding a breast with the patient lying in the prone position. Each antenna in turn illuminates the breast and the multistatic returns are recorded. A delay and sum beamforming algorithm is used to process the returns and create an intermediate image of the breast. The antenna array is then rotated counter-clockwise around the breast so the new location of the i th antenna is half way between the previous location of the i th and $(i + 1)$ th antennas, as shown in Figure 2. The breast is once again illuminated by UWB pulses and the multistatic signals are recorded. These signals are beamformed to create a second intermediate image. These intermediate images are then multiplied pixel-by-pixel to create a final resultant image.

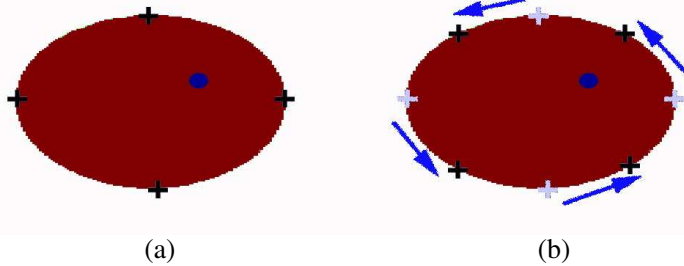


Figure 2. The original antenna configuration, used to create the first intermediate image, is shown in Figure 2(a). The antennas are then rotated to create the second image, as shown in Figure 2(b). A tumor is located in the top-right quadrant.

4. TEST PROCEDURES AND RESULTS

4.1. 2D FDTD Models and Performance Metric

A 2D Finite Difference Time Domain (FDTD) breast model was developed, based on a patient lying in the prone position with a circular array of antenna surrounding the breast. The model is based on an MRI-derived breast phantom, taken from the UWCEM breast phantom repository at the University of Wisconsin, Madison [37]. These phantoms are derived from T1-weighted MR images of the breast, with each voxel within the phantom assigned appropriate dielectric properties, based on previous dielectric studies by Lazebnik et al. [31,32]. This method preserves the structural heterogeneity of the breast and the highly correlated nature of fibroglandular tissue distribution in the breast, as opposed to other methods that model the variation of dielectric properties as being randomly distributed. In two dimensions, a coronal slice of breast is considered, as shown in Figure 3. The antenna array consists of a number of elements (numbering from 4 to 20) modelled as electric-current sources, equally spaced around the circumference of the breast, and placed close to the skin. The antenna array is backed by a synthetic material matching the dielectric properties of skin. Two sizes of tumors are used to test the rotating antenna system, 6 mm and 10 mm in diameter. A location within the breast is described in terms of (X mm, Y mm). A tumor is positioned at four different locations within the breast (45 mm, 35 mm), (45 mm, 50 mm), (20 mm, 50 mm) and (20 mm, 35 mm). The input signal is a 150-ps differentiated Gaussian pulse, with a centre frequency of 7.5 GHz and

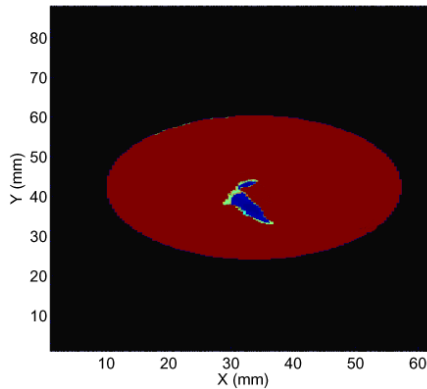


Figure 3. FDTD model of the breast taken from the UWCEM breast phantom repository at the University, of Wisconsin, Madison [37]. The adipose (fatty) breast tissue is shown in red, while the fibroglandular tissue is highlighted in blue.

a -3dB bandwidth of 9 GHz. An idealized artifact removal algorithm, as previously described by Bond et al. [38] is used to remove the input signal and the reflection from the skin-breast interface. The artifact to be removed is established by measuring the backscattered signals from a homogeneous FDTD model with no tumor present. These signals are then subtracted channel-by-channel from the with-tumor responses. Finally, since the input signal is a differentiated Gaussian pulse with a zero crossing at its centre point, the backscattered signal from any dielectric scatterer would also have a zero crossing at its centre point. In order to overcome this, the signals are integrated to produce a maximum at the centre point.

The Signal-to-Mean Ratio (SMR) [39] is used to evaluate the robustness and performance of rotating antenna system. The SMR compares the maximum tumor response with the mean response of the different tissues across the breast in the same image of backscattered energy [39].

4.2. Results

Seventy-two FDTD simulations were completed, with two different-sized tumors positioned at four different locations within the breast (one location in each quadrant). The number of antennas surrounding the breast was varied from 4 to 20. An initial image of the breast was created (using a multistatic delay and sum beamformer). The antennas

were then rotated and a second image was created; this second image represents the output of a multistatic system with a slightly different static antenna configuration to the first image. The two images were then multiplied pixel-by-pixel and then the resulting image was compared to the two images from the two individual static antenna configurations. The SMR was calculated for each simulation and the results are shown in Figure 4. It can be seen that the rotating antennas approach considerably outperformed the fixed antenna system across all tests. In particular, the improvement in SMR of the rotating antenna system when compared to the fixed antenna system ranged from 10–16 dBs. Significantly, even when twenty antennas are used,

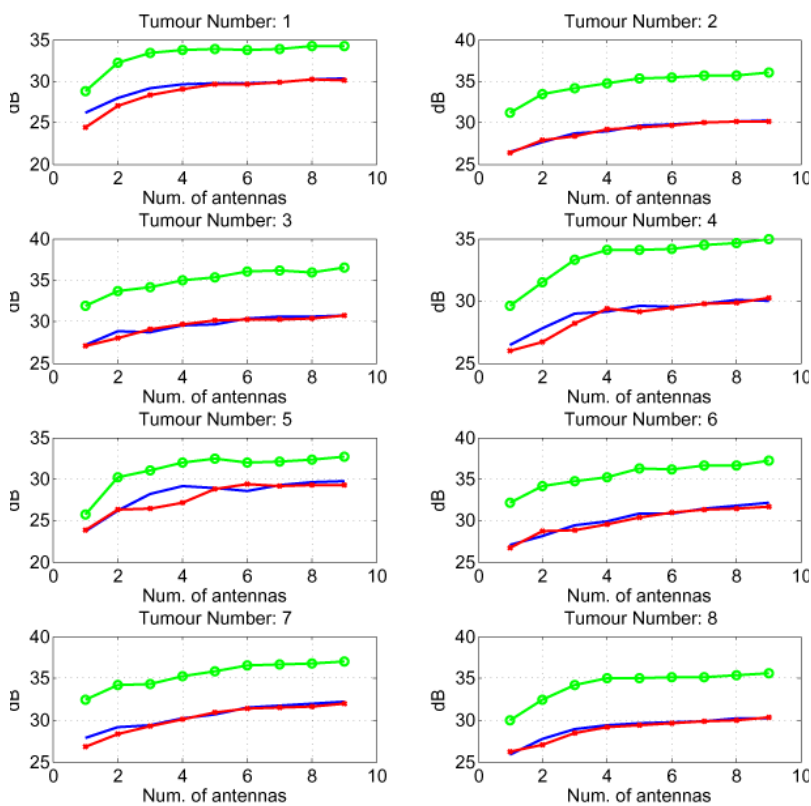


Figure 4. Comparison of SMR plotted as a function of the number of antennas in the array for the two intermediate images (shown in blue and red) and the combined image shown in green. The results for eight tumour size/positions are shown.

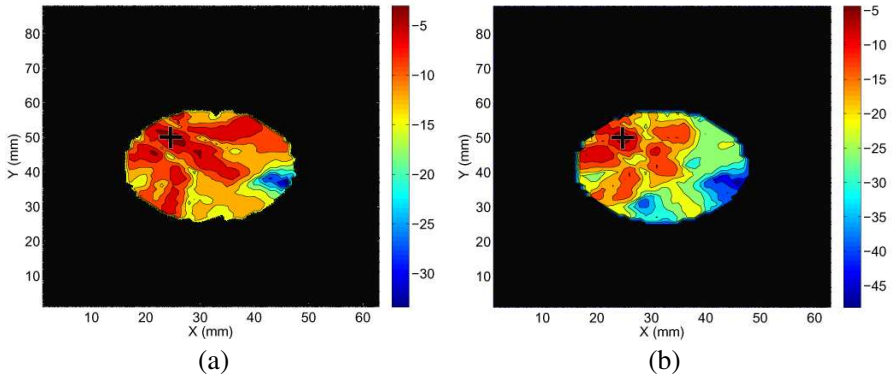


Figure 5. Comparison of image created using fixed (a) and rotating antenna system (b) using 4 antennas. A black cross indicates the location of the tumor. Note the different dB scales on each image, highlighting the improved clutter suppression ability of the rotating antenna system.

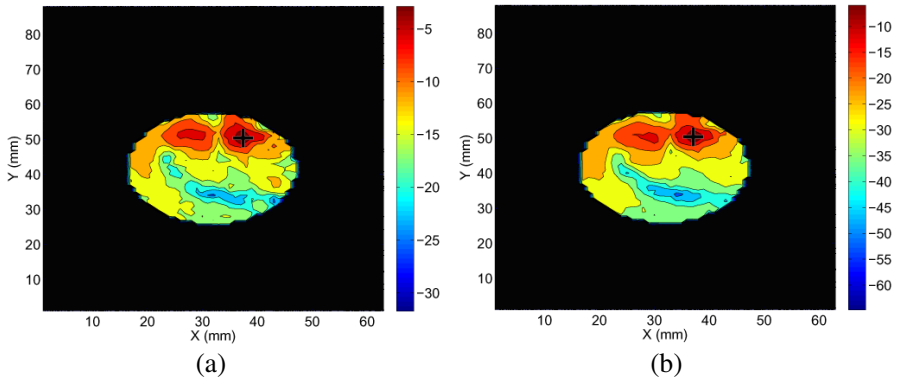


Figure 6. Comparison of image created using fixed (a) and rotating antenna system (b) using 16 antennas. A black cross indicates the location of the tumor. Note the different dB scales on each image, highlighting the improved clutter suppression ability of the rotating antenna system.

almost covering the entire surface of the breast, the rotating antenna algorithm still outperforms the fixed antenna system.

In addition to the quantitative results presented in Figure 4, several sample images are also shown for comparison. Images created by the fixed antenna and rotating antenna system are shown in

Figure 5, created using four antennas. The position and location of the tumor is much more clearly visible in the image produced by the rotating antenna system. The increased clutter-suppression ability of the rotating antenna system is also clearly evident in the resultant images (note the different dB scale on each image). Finally, a second set of images is presented in Figure 6, created using sixteen antennas. Once again the images are shown side-by-side for direct comparison, and tumor response is much stronger (compared to the background clutter due to dielectric heterogeneity) in the image produced by the rotating antenna system.

5. CONCLUSIONS AND FUTURE WORK

Multistatic UWB imaging algorithms have previously been shown to significantly outperform monostatic systems for two specific reasons:

- The spatial diversity of the multistatic transmit and receive antenna allow for improved localisation of any tumors within the breast.
- The extra signals recorded using the multistatic approach provide for an improved breast image when coherent addition of the returns is achieved.

In this paper, a rotating antenna system is presented which seeks to further increase the number of unique multistatic signals by rotating the antenna array around the breast. An intermediate image is created using the delay and sum beamformer with the antennas in one fixed configuration. The antenna array is then rotated and a second independent image is created. Finally, these two image are multiplied pixel-by-pixel to create the final combined image. The rotating antenna system is evaluated on a 2D MRI-derived breast phantom from the UWCEM breast phantom repository [37]. Eight tumor positions/sizes are considered, and images are created using both the fixed antenna array (with a delay and sum beamformer) and the rotating antenna array system. Furthermore, each simulation is repeated with antenna numbers ranging from 4 to 20 in steps of two antennas. In every case considered, the rotating antenna system significantly outperformed the existing fixed antenna system in terms of SMR. The improvement offered by the rotating antenna system is also qualitatively evident in the resultant images. The increased performance of the rotating array system is due to the extra multistatic signals acquired when the antenna array is rotated. It must also be acknowledged that some of the performance improvement offered by the rotating antenna system is due to the multiplicative processing of the individual independent

images. Future work will involve evaluating the algorithm using 3D simulations and using an experimental breast phantom.

ACKNOWLEDGMENT

This work is supported by Science Foundation Ireland (SFI) under grant number 07/RFP/ENEF420.

REFERENCES

1. Nass, S. L., I. C. Henderson, and J. C. Lashof, *Mammography and Beyond: Developing Technologies for the Early Detection of Breast Cancer*, National Academy Press, 2001.
2. Wang, L., X. Zhao, H. Sun, and G. Ku, "Microwave-induced acoustic imaging of biological tissues," *Rev. Sci. Instrum.*, Vol. 70, No. 9, 3744–3748, 1991.
3. Li, D., P. M. Meaney, T. Raynolds, S. A. Pendergrass, M. W. Fanning, and K. D. Paulsen, "Parallel-detection microwave spectroscopy system for breast cancer imaging," *Rev. Sci. Instrum.*, Vol. 75, No. 7, 2305–2313, 2004.
4. Kruger, R. A., K. D. Miller, H. E. Reynolds, W. L. Kiser, D. R. Reinecke, and G. A. Kruger, "Breast cancer in vivo: Contrast enhancement with thermoacoustic CT at 434 MHz — Feasibility study," *Radiology*, Vol. 216, No. 1, 279–283, 2000.
5. Bulyshev, A., S. Y. Semenov, A. E. Souvorov, R. H. Svenson, A. G. Nazorov, Y. E. Sizov, and G. P. Tatis, "Computational modeling of three-dimensional microwave tomography of breast cancer," *IEEE Trans. Biomed. Eng.*, Vol. 48, No. 9, 1053–1056, Sep. 2001.
6. Meaney, P. M., M. W. Fanning, D. Li, S. P. Poplack, and K. D. Paulsen, "A clinical prototype for active microwave imaging of the breast," *IEEE Trans. Microwave Theory Tech.*, Vol. 48, No. 11, 1841–1853, Nov. 2000.
7. Meaney, P. M., K. D. Paulsen, J. T. Chang, M. W. Fanning, and A. Hartov, "Nonactive antenna compensation for fixed-array microwave imaging: Part II -Imaging results," *IEEE Trans. Med. Imag.*, Vol. 18, No. 6, 508–518, Jun. 1999.
8. Souvorov, A. E., A. E. Bulyshev, S. Y. Semenov, R. H. Svenson, and G. P. Tatis, "Two-dimensional analysis of a microwave flat antenna array for breast cancer tomography," *IEEE Trans. Microwave Theory Tech.*, Vol. 48, No. 8, 1413–1415, Aug. 2000.

9. Bulyshev, A. E., S. Y. Semenov, A. E. Souvorov, R. H. Svenson, A. G. Nazarov, Y. E. Sizov, and G. P. Tatsis, "Computational modeling of three-dimensional microwave tomography of breast cancer," *IEEE Trans. Biomed. Eng.*, Vol. 48, No. 9, 1053–1056, Sep. 2001.
10. Liu, Q. H., Z. Q. Zhang, T. Wang, J. A. Byran, G. A. Ybarra, L. W. Nolte, and W. T. Joines, "Active microwave imaging i — 2-D forward and inverse scattering methods," *IEEE Trans. Microwave Theory Tech.*, Vol. 50, No. 1, 123–133, Jan. 2002.
11. Hagness, S. C., A. Taflove, and J. E. Bridges, "Two-dimensional FDTD analysis of a pulsed microwave confocal system for breast cancer detection: Fixed-focus and antenna-array sensors," *IEEE Trans. Biomed. Eng.*, Vol. 45, No. 12, 1470–1479, 1998.
12. Hagness, S. C., A. Tatlove, and J. E. Bridges, "Three-dimensional FDTD analysis of a pulsed microwave confocal system for breast cancer detection: Design of an antennaarray element," *IEEE Trans. Antennas and Propagat.*, Vol. 47, No. 5, 783–791, May 1999.
13. Fear, E. C., X. Li, S. C. Hagness, and M. A. Stuchly, "Confocal microwave imaging for breast cancer detection: Localization of tumors in three dimensions," *IEEE Trans. Biomed. Eng.*, Vol. 49, No. 8, 812–822, Aug. 2002.
14. Fear, E. C. and M. A. Stuchly, "Microwave system for breast tumor detection," *IEEE Microwave and Guided Wave Letters*, Vol. 9, No. 11, 470–472, Nov. 1999.
15. Fear, E. C., J. Sill, and M. A. Stuchly, "Experimental feasibility study of confocal microwave imaging for breast tumor detection," *IEEE Trans. Microwave Theory Tech.*, Vol. 51, No. 3, 887–892, Mar. 2003.
16. Fear, E., J. Sill, and M. Stuchly, "Microwave system for breast tumor detection: Experimental concept evaluation," *IEEE AP-S International Symposium and USNC/URSI Radio Science Meeting*, Vol. 1, 819–822, San Antonio, Texas, Jun. 2002.
17. Li, X. and S. C. Hagness, "A confocal microwave imaging algorithm for breast cancer detection," *IEEE Microwave and Wireless Components Letters*, Vol. 11, No. 3, 130–132, 2001.
18. Li, X., E. J. Bond, B. D. V. Veen, and S. C. Hagness, "An overview of ultra-wideband microwave imaging via space-time beamforming for early-stage breast-cancer detection," *IEEE Antennas and Propagation Magazine*, Vol. 47, No. 1, 19–34, Feb. 2005.
19. Hernandez-Lopez, M., M. Quintillan-Gonzalez, S. Garcia, A. Bretones, and R. Martin, "A rotating array of antennas for

- confocal microwave breast imaging," *Microw. Opt. Technol. Lett.*, Vol. 39, No. 4, 307–311, Nov. 2003.
20. De Rodriguez, M., M. Vera-Isasa, and V. S. del Rio, "3-D microwave breast tumor detection: Study of system performance," *IEEE Trans. Biomed. Eng.*, Vol. 55, No. 12, 2772–2777, 2008.
 21. O'Halloran, M., M. Glavin, and E. Jones, "Channel-ranked beamformer for the early detection of breast cancer," *Progress In Electromagnetics Research*, Vol. 103, 153–168, 2010.
 22. O'Halloran, M., M. Glavin, and E. Jones, "Effects of fibroglandular distribution on data-independent beamforming algorithms," *Progress In Electromagnetics Research*, Vol. 97, 141–158, 2009.
 23. O'Halloran, M., M. Glavin, and E. Jones, "Quasi-multistatic MIST beamforming for the early detection of breast cancer," *IEEE Trans. Biomed. Eng.*, Vol. 57, No. 4, 830–40, 2009.
 24. Lazaro, A., D. Girbau, and R. Villarino, "Simulated and experimental investigation of microwave imaging using UWB," *Progress In Electromagnetics Research*, Vol. 94, 263–280, 2009.
 25. Lazaro, A., D. Girbau, and R. Villarino, "Wavelet-based breast tumor localization technique using a UWB radar," *Progress In Electromagnetics Research*, Vol. 98, 75–95, 2009.
 26. Zhang, H., S. Y. Tan, and H. S. Tan, "A novel method for microwave breast cancer detection," *Progress In Electromagnetics Research*, Vol. 83, 413–434, 2008.
 27. Bindu, G., S. J. Abraham, A. Lonappan, V. Thomas, C. K. Aanandan, and K. T. Mathew, "Active microwave imaging for breast cancer detection," *Progress In Electromagnetics Research*, Vol. 58, 149–169, 2006.
 28. Joines, W. T., Y. Zhang, C. Li, and R. L. Jirtle, "The measured electrical properties of normal and malignant human tissues from 50 to 900 MHz," *Med. Phys.*, Vol. 21, No. 4, 547–550, Apr. 1994.
 29. Surowiec, A. J., S. S. Stuchly, J. R. Barr, and A. Swarup, "Dielectric properties of breast carcinoma and the surrounding tissues," *IEEE Trans. Biomed. Eng.*, Vol. 35, No. 4, 257–263, Apr. 1988.
 30. Chaudhary, S. S., R. K. Mishra, A. Swarup, and J. M. Thomas, "Dielectric properties of normal and malignant human breast tissue at radiowave and microwave frequencies," *Indian J. Biochem. Biophys.*, Vol. 21, 76–79, 1984.
 31. Lazebnik, M., L. McCartney, D. Popovic, C. B. Watkins, M. J. Lindstrom, J. Harter, S. Sewall, A. Magliocco, J. H. Booske,

- M. Okoniewski, and S. C. Hagness, "A large-scale study of the ultrawideband microwave dielectric properties of normal breast tissue obtained from reduction surgeries," *Phys. Med. Biol.*, Vol. 52, 2637–2656, 2007.
32. Lazebnik, M., D. Popovic, L. McCartney, C. B. Watkins, M. J. Lindstrom, J. Harter, S. Sewall, T. Ogilvie, A. Magliocco, T. M. Breslin, W. Temple, D. Mew, J. H. Booske, M. Okoniewski, and S. C. Hagness, "A large-scale study of the ultrawideband microwave dielectric properties of normal, benign and malignant breast tissues obtained from cancer surgeries," *Phys. Med. Biol.*, Vol. 52, 6093–6115, 2007.
 33. Shea, J. D., P. Kosmas, S. C. Hagness, and B. D. V. Veen, "Contrast-enhanced microwave imaging of breast tumors: A computational study using 3d realistic numerical phantoms," *Inverse Problems*, Vol. 26, 2010.
 34. O'Halloran, M., R. Conceicao, D. Byrne, M. Glavin, and E. Jones, "FDTD modeling of the breast: A review," *Progress In Electromagnetics Research B*, Vol. 18, 1–24, 2009.
 35. Campbell, A. M. and D. V. Land, "Dielectric properties of female human breast tissue measured in vitro at 3.2 GHz," *Phys. Med. Biol.*, Vol. 37, No. 1, 193–210, 1992.
 36. Meaney, P. M., M. W. Fanning, D. Li, S. P. Poplack, and K. D. Paulsen, "A clinical prototype for active microwave imaging of the breast," *IEEE Trans. Microwave Theory Tech.*, Vol. 48, 1841–1853, 2000.
 37. UWCEM, (Last accessed: June. 2010), UWCEM Numerical Breast Phantoms Repository, [Online], available: <http://uwcem.ece.wisc.edu/home.htm>.
 38. Bond, E. J., X. Li, S. C. Hagness, and B. D. V. Veen, "Microwave imaging via space-time beamforming for early detection of breast cancer," *IEEE Trans. Antennas and Propagat.*, No. 8, 1690–1705, Aug. 2003.
 39. Conceição, R. C., M. O'Halloran, M. Glavin, and E. Jones, "Antenna configurations for ultra wide band radar detection of breast cancer," *Progress in Biomedical Optics and Imaging*, Vol. 10, No. 9, 7169, 2009.